Chinese Chemical Letters 35 (2024) 108644

Contents lists available at ScienceDirect

Chinese Chemical Letters

journal homepage: www.elsevier.com/locate/cclet

In situ crosslink polymerization induced long-lived multicolor supramolecular hydrogel based on modified β-cyclodextrin☆

Yonghui Sun[1], Linnan Jiang[1], Yong Chen, Yu Liu*

College of Chemistry, State Key Laboratory of Elemento-Organic Chemistry Nankai University, Tianjin 300071, China

ARTICLE INFO

Article history:
Received 30 March 2023
Revised 26 May 2023
Accepted 2 June 2023
Available online 3 June 2023

Keywords:
Room temperature phosphorescence
Hydrogel
Phosphorescence energy transfer
Cyclodextrin
Supramolecular interaction

ABSTRACT

The construction of hydrogels with good mechanical properties and phosphorescent properties is full of challenges. Herein, we report a supramolecular phosphorescent hydrogel with long lifetime, high tensile strength and self-healing property, which can be easily constructed through *in-situ* thermal-initiated polymerization of isocyanatoethyl acrylate-modified β-cyclodextrin (β-CD-DA) and acrylate-modified adamantane (Ad-DA), acrylic acid (AA), followed by the non-covalent association with carbon dots (CNDs). The lifetime of phosphorescent hydrogel can reach 1261 ms at room temperature, and the quantum yield is 11%. Importantly, through the efficient triplet to singlet Förster resonance energy transfer (TS-FRET), the phosphorescent hydrogel shows the good phosphorescence energy transfer property for organic dyes Rhodamine B and Eosin Y with the delayed fluorescence lifetime up to 730 ms and 585 ms as well as the energy transfer efficiency (Φ_{ET}) up to 99.9% and 99.3%, respectively. Moreover, owing to the host-guest interactions between β-CD-DA and Ad-DA, the three-dimensional cross-linked network phosphorescent hydrogel can be easily stretched to 18 times of its original length, and can achieve self-healing of the cut surfaces within 30 min. These results will expand the scope of phosphorescent materials and provide new ideas and opportunities for materials science.

Room temperature phosphorescent (RTP) materials, with their unprecedented photophysical properties, such as long lifetime, rich triplet excitons and large Stokes shift, have shown great application prospects in the fields of information anti-counterfeiting, information storage and biological imaging [1–8]. Among them, hydrogel materials attracted more and more attentions in the field of RTP materials due to their large water content, high deformability and recoverability [9,10]. However, due to the fact that the triplet excitons are easily deactivated by the invasion of moisture and oxygen under ambient conditions, it is still a great challenge to achieve efficient and long-lived RTP emission in the hydrogel phase [11–14]. In recent years, a series of interesting RTP systems have been designed and developed based on the idea of enhancing the intersystem crossing process and suppressing the nonradiative decay [15–18]. For example, George and co-workers recently reported the room temperature phosphorescence using an organic-inorganic supramolecular scaffolding strategy, which achieved the high phosphorescence quantum yield in solution and gel phase under environmental conditions [10]. In addition, many excellent strategies, including crystallization, host-guest doping, and polymerization, are also used to effectively enhance the RTP emission [19–22]. Regrettably, most of RTP materials can only emit afterglow in the form of crystals or rigid host-guest systems, which greatly hinders their practical application [23–25]. To the best of our knowledge, long-lived supramolecular phosphorescent hydrogels with good mechanical properties and luminescent properties have not been reported yet.

As a promising candidate for metal-free RTP materials, carbon nanodots (CNDs) have made great progress since 2013 due to their excellent photophysical properties, good biocompatibility, high stability as well as low toxicity, and have been widely used in bioimaging, sensing and optoelectronic devices [26–28]. Recently, Shan and co-workers have shown that the ultralong and efficient phosphorescence emission of water-soluble CNDs is achieved by confine CNDs to the silica capsulation layer [29]. On the other hand, the host-guest supramolecular interactions based on cyclodextrins (CDs) have received extensive attention in the field of supramolecular gels [29–35]. Harada *et al.* reported several functional properties of CD-based supramolecular polymers, including macroscopic self-assembly, self-healing ability and biomedical applications [36–41]. Zhang *et al.* reported the antibacterial

☆ This paper is dedicated to the memory of Prof. Jiang Wei.

* Corresponding author.
E-mail address: yuliu@nankai.edu.cn (Y. Liu).

[1] These authors contributed equally to this work.

https://doi.org/10.1016/j.cclet.2023.108644
1001-8417/

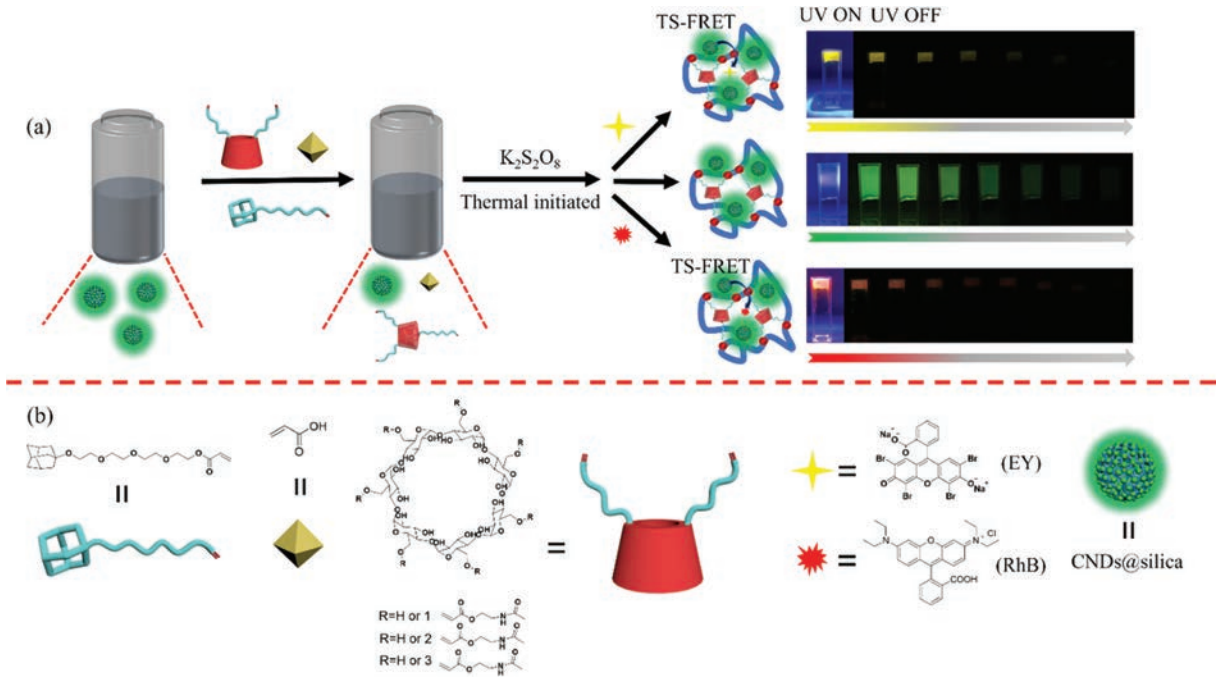

Scheme 1. (a) Construction of the multicolor supramolecular phosphorescent hydrogel. Inset: the green phosphorescence and delay fluorescence photographs of supramolecular hydrogel after withdrawing 365 nm UV lamp. TS-FRET represents room-temperature phosphorescence energy transfer. (b) Molecular structures of C=C bond modified β-cyclodextrin (β-CD-DA) and adamantane (Ad-DA), acrylic acid (AA) and fluorescent molecule EY and RhB.

wound-dressings with self-healing property that can effectively improve the wound repairing ratio through host-guest complexation of modified cyclodextrin and adamantane [42]. Wang *et al.* designed cyclodextrin and adamantane derivatives with C=C bond at the end and copolymerized them with gelatin-methacryloyl to enhance the mechanical properties and further prepared self-healing hydrogels suitable for 3D printing [43]. Therefore, it is widely regarded that the combination of CNDs with CD-based supramolecular hydrogel system can lead to the flexible supramolecular phosphorescent nanomaterials with tensile, self-healing and luminescent properties. This organic-inorganic hybrid supramolecular active hydrogel strategy may provide effective and environmentally sustainable alternatives to optical materials, and inspire new ideas for phosphorescent materials.

Herein, we have developed a kind of multicolor supramolecular intelligent hydrogel with ultralong phosphorescence, high tensile strength and self-healing properties through *in-situ* thermal-initiated polymerization using the organic-inorganic hybrid strategy (Scheme 1a). The hydrogel can emit the green phosphorescence excited by 365 nm UV lamp, with an afterglow up to 10 s at room temperature and a lifetime of 1261 ms. Significantly, the hydrogel network can be easily stretched to 18 times its original length and reversibly and quickly recovered. Owing to the host-guest interactions of β-CD and adamantane, the hydrogel can be rapidly self-heal after being cut into pieces. In addition, this phosphorescent hydrogel exhibited the good phosphorescence energy transfer for fluorescent dyes Rhodamine B (RhB) and Eosin Y (EY) through an efficient TS-FRET process, showing the high energy transfer efficiency (Φ_{ET}) of 99.9% and 99.3%, respectively. The delayed fluorescence lifetime of acceptor molecule can also reach 730 ms and 585 ms respectively, which is rarely reported in hydrogel phase. District from crystalline phosphorescence materials, this kind of supramolecular intelligent phosphorescent material not only integrates the light emitting properties, gel properties and biocompatibility but also is easy to be fabricated into large-scale, which enables a bright application prospect.

To achieve long-lived phosphorescence emission in hydrogel phase, it is necessary to find suitable water-soluble phosphor groups. According to the report by Shan *et al.*, CNDs were synthesized from ethylenediamine and phosphoric acid *via* a microwave method (Scheme S1 in Supporting information). High resolution transmission electron microscope (TEM) images showed the *quasi*-spherical shape of CNDs with an average diameter of about 5 nm, and the lattice spacing of 0.2 nm corresponded to the D-spacing of graphene (100) planes (Figs. S1 and S2 in Supporting information). The amorphous morphology of CNDs was characterized by powder X-ray diffraction, and the main peak of 23.56° was attributed to the (002) planes of graphitic carbon (Fig. S3 in Supporting information). The Raman spectra of CNDs showed two peaks at 1315 cm^{-1} and 1545 cm^{-1}, assigned to the disordered and graphite carbon with a ratio of 0.82 (Fig. S4 in Supporting information). Such a small ratio means that an ordered carbon core was formed in CNDs. Then, CNDs aqueous solution was premixed with ammonia and tetraethoxysilane. As shown in Fig. 1a, TEM of the premixed CNDs aqueous solution shows that the nanoparticles are coated by amorphous silica shells. Due to the confinement of the silica shell, the phosphorescence of CNDs is prevented from being quenched by the invasion of water and oxygen, thus achieving an ultralong water soluble phosphorescent CNDs@silica system. The steady-state and delayed (at fixed delay of 100 μs) emission spectra of CNDs@silica were measured (Figs. S5 and S6 in Supporting information). The emission band at 520 nm was determined as the phosphorescent radiation decay channel with a lifetime of 1704 ms and a quantum yield of 8% (Figs. S7–S9 and Video S1 in Supporting information). On the other hand, through a nucleophilic addition reaction, the end of β-CD is randomly modified by C=C bond to form β-CD-DA that were characterized by ^{1}H NMR spectroscopies and HR-MS (Figs. S10 and S11 in Supporting information). In the ^{1}H NMR spectrum, the ratio of signal integral area of C1-H of β-CD to that of C=C bond is 7:6, indicating that there are about two double bonds in each β-CD-DA. Then, as the guest molecule, the C=C bond modified adamantane (Ad-DA) was syn-

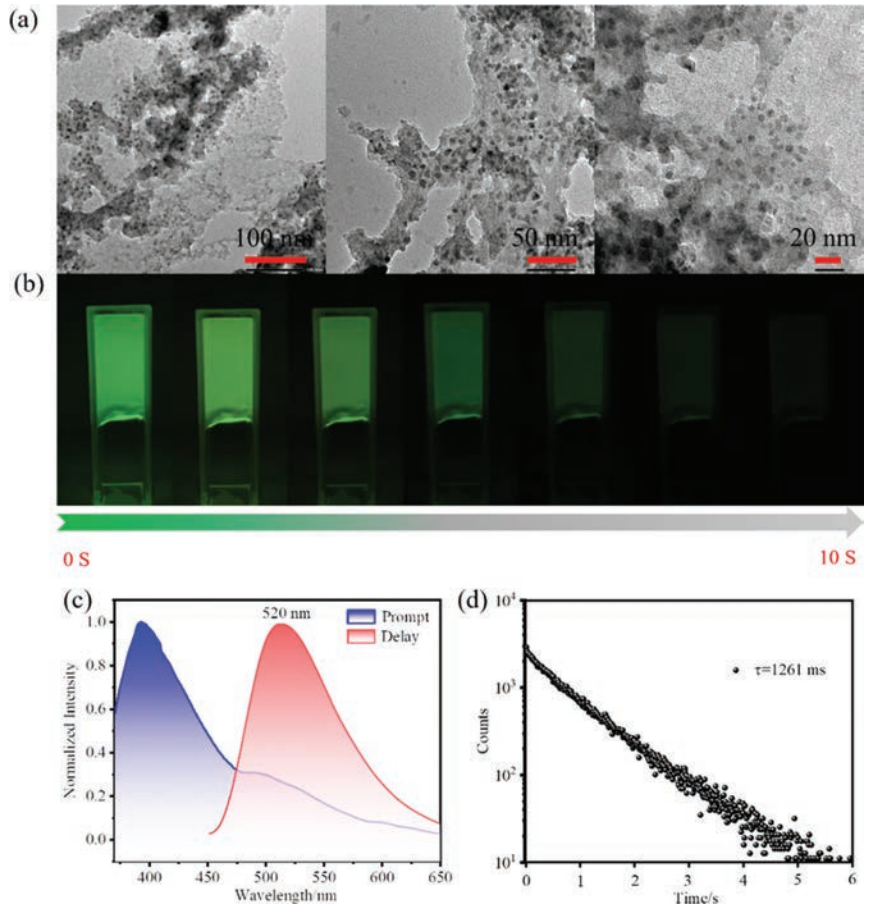

Fig. 1. (a) TEM images of CNDs@silica. (b) The photographs of hydrogel after UV irradiation. (c) Prompt and delayed phosphorescence spectra of hydrogel. Excitation by 343 nm, delayed time: 1000 μs. (d) Lifetime decay curve of hydrogel collected at 520 nm.

thesized through two simple steps (Scheme S2 in Supporting information). To investigate the complexation behavior between β-CD-DA and Ad-DA, we employed Ad-DA as a guest and β-CD-DA as a host for the ^{1}H NMR titration experiment. As shown in the Fig. S12 (Supporting information), with the equivalent of β-CD-DA increased from 0 to 2.5, NMR signals of H_a protons on Ad-DA showed an obvious down-field shifts from 2.13 ppm to 2.3 ppm, indicating that adamantane entered the β-CD cavity to form host-guest complexes. By analyzing the non-linear least square fitting of titration data, the binding constant of Ad-DA to β-CD-DA was determined to be 8.94×10^4 L/mol, and the stoichiometric ratio was determined as 1:1 (Figs. S13 and S14 in Supporting information). In addition, the 2D ROESY NMR spectrum of Ad-DA and β-CD-DA exhibited an obvious NOE effect between interior protons in the cavity of β-CD and protons of adamantane, which further indicates the inclusion of Ad-DA in the β-CD-DA cavity (Fig. S15 in Supporting information).

In order to prepare supramolecular phosphorescent hydrogel, we introduced acrylic acid (AA), Ad-DA and β-CD-DA into CNDs@silica aqueous solution matrix. Among them, acrylic acid, as the main component of polymerization can also adjust the pH of CNDs@silica aqueous solution because neutral environment is more conducive to the formation of hydrogel. On the other hand, unlike the polymerization of Ad-DA and β-CD-DA, the introduction of acrylic acid enhances the flexibility of the hydrogel. The CNDs@silica aqueous solution containing supramolecular assembly Ad-DA/β-CD-DA ([Ad-DA] = [β-CD-DA] = 0.1 mmol/mL) and AA ([AA]=3.4 mmol/mL) was obtained by simply stirring the components mentioned above. Subsequently, in the presence of $K_2S_2O_8$, the luminescent materials CNDs@silica-[Ad-DA/β-CD-DA/AA] hydrogel was be obtained by thermal polymerization for 30 min. To our surprise, the hydrogel still retains the good luminescent properties of CNDs@silica even after experiencing a complex polymerization process. As shown in Figs. 1c and d, the steady-state and delayed (at fixed delay of 1000 μs) emission spectra of the supramolecular hydrogel showed the fluorescence emission band at 392 nm and the phosphorescence emission band at 520 nm. The phosphorescence lifetime and quantum yield at room temperature are 1261 ms and 11.31% respectively (Fig. S16 in Supporting information), and the bright long afterglow up to tens of seconds can be observed with the naked eye (Fig. 1b and Video S2 in Supporting information). Compared with the aqueous solution of CNDs@silica, the quantum yield of the gel phase increased by about 3%, and the afterglow time increased by about 2 s.

To achieve an effective phosphorescence capture system in hydrogel phase, we investigate the possibility of doping fluorescent dyes into supramolecular cross-linking networks through *in-situ* thermal polymerization to achieve the spatial compactness of donor and acceptor molecules. We selected CNDs@silica as the energy donor. EY or RhB with high fluorescence quantum yield and good spectral overlap with the CNDs@silica phosphorescence emission were selected as the acceptors (Fig. 2a). As depicted in Fig. 2b, as the fraction of EY in the hydrogel gradually increases, the green phosphorescence emission band of CNDs@silica at 520 nm gradually decreases until the fraction of EY reaches 2.66%. The phosphorescence emission band of the hydrogel at 520 nm disappeared at this time, and the delay emission spectra (at fixed delay of 100 μs) only showed the emission band at 565 nm, which is consis-

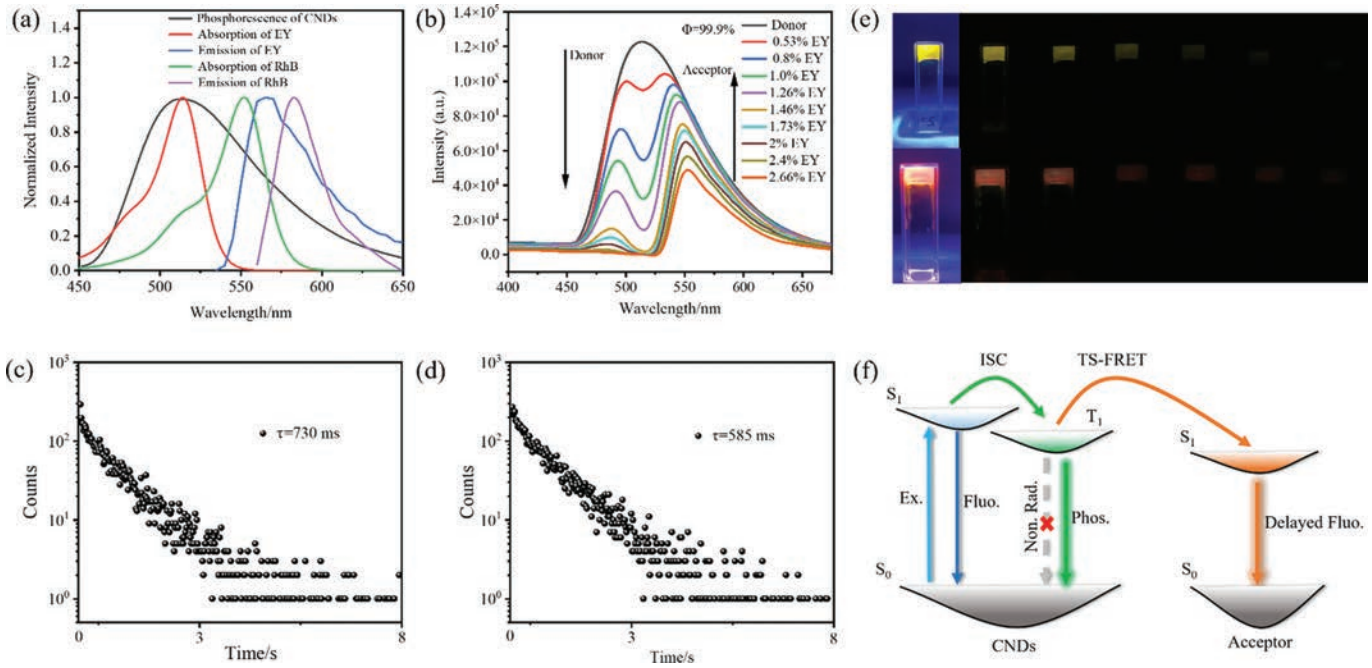

Fig. 2. (a) Normalized emission spectrum of CNDs@silica, EY, RhB and absorption spectra of EY and RhB. (b) Phosphorescence emission spectra (100 μs delay) of hydrogel at different donor/acceptor ratios at 298 K ([Ad-DA] = [β-CD-DA] = 0.1 mmol/mL, [AA] = 3.4 mmol/mL, λ_{ex} = 343 nm). (c, d) Lifetime decay curve of hydrogel collected at 565 and 590 nm respectively. (e) The photographs of delay fluorescence after UV irradiation. (f) Diagram of the possible mechanism for RTP energy transfer process (Ex. = excitation, Fluo. = fluorescence, Non. Rad. = non-radiation, Phos. = phosphorescence, ISC = intersystem crossing, TS-FRET = triplet-to-singlet Förster resonance energy transfer).

tent with the fluorescence of EY, indicating the delayed sensitization process and TS-FRET. Interestingly, the delayed fluorescence emission in the hydrogel at 565 nm has a lifetime of 730 ms and displays a bright yellow afterglow of 7 s at room temperature (Figs. 2c and e, Video S3 in Supporting information), which is completely different from the fluorescence lifetime of EY at nanosecond level. The quantum yield of the hydrogel reached 20.57% (Fig. S17 in Supporting information). In addition, the energy transfer efficiency has reached 99.9%, which is the highest energy transfer efficiency in the hydrogel phase so far (The energy transfer efficiency is calculated by Eq. S1 in Supporting information). Moreover, we also investigated the photophysical property of hydrogels when RhB was used as an acceptor. As shown in Fig. S18 (Supporting information), with the gradual increase of the fraction of RhB in the hydrogel, the phosphorescence emission at 520 nm in the delay spectra quenched rapidly, but the fluorescence at 590 nm increased. The lifetime of delayed fluorescence was measured to be 585 ms, accompanied by a red afterglow of about 6 s under the excitation of 365 nm (Figs. 2d and e, Video S4 in Supporting information). This significant delayed fluorescence emission can be observed with the naked eye, indicating an effective phosphorescent energy transfer from donor to acceptor. In addition, the quantum yield of the hydrogel was measured as 20.66%, and the energy transfer efficiency reached 99.3% (Fig. S19 in Supporting information). Fig. 2f showed the possible mechanism of phosphorescence-capturing system. Due to the large spectral overlap with EY and RhB, the dipole oscillation of phosphorescence hydrogel under direct excitation can cause the change of EY or RhB dipole distribution, leading to the effective energy transfer between donor and acceptor.

Considering that the supramolecular cross-linked networks may provide an energy-dissipation mechanism for the hydrogel to buffer the applied internal stress, we further explored the mechanical property of the obtained self-standing supramolecular phosphorescent hydrogel. Two phosphorescent hydrogels with different concentrations of Ad-DA/β-CD-DA assembly ([Ad-DA] = [β-CD-DA] = 0.1 mmol/mL, 0.05 mmol/mL) were prepared. From the SEM images of their freeze-dried hydrogels, clear three-dimensional porous network structures were observed (Fig. S20 in Supporting information). Such a microstructure was expected because Ad-DA/β-CD-DA assembly could readily form cross-linked network during polymerization with acrylic acid. The mechanical property of the hydrogel was studied by tensile test. The results of stress-strain curves showed that 0.05 mmol/mL phosphorescent hydrogel could be easily stretched to 3500% of its original length (Fig. 3a), but the strength and recovery properties of hydrogel were poor, and the plastic deformation accounts for a large proportion (30%) in the stretching process (Fig. S21 in Supporting information). In contrast, the phosphorescent hydrogel with higher cross-linking density ([Ad-DA] = [β-CD-DA] =0.1 mmol/mL) exhibited a larger modulus, which can not only stretch to 1800% of its original length, but also have more than 85% strain recovery (Figs. 3a and b). The hysteresis loop area of this hydrogel is much smaller than that of 0.05 mmol/mL hydrogel. It is worth noting that even after 5 loading-unloading cycles, the hydrogel remained in its original condition without any damage on the surface (Fig. S22 in Supporting information). To explore optical properties of hydrogel ([Ad-DA] = [β-CD-DA] = 0.1 mmol/mL) under external force, we tested its phosphorescence spectrum at tensile strain of 700%, and the results showed that the phosphorescence intensity of the hydrogel was weakened (Fig. S23 in Supporting information). In addition, the elasticity of the hydrogel doped with EY or RhB were tested at a concentration of 0.1 mmol/mL Ad-DA/β-CD-DA assembly. As shown in Fig. 3c, the hydrogel can be stretched to 1600% and 1580% of its original length, respectively. Moreover, both hydrogels have more than 90% strain recovery in the loading-unloading cycle experiment (Figs. S24 and S25 in Supporting information). These results showed that due to the reversibility of host-guest interactions, these hydrogels showed the good fatigue-resistant and elasticity. By calculating the fracture energy, the relative maximum fracture energy of the hydrogel with 0.1 mmol/mL concentration Ad-DA/β-CD-DA assembly is 13.5 MJ/m^3, followed by the fracture energy of the hydrogel with

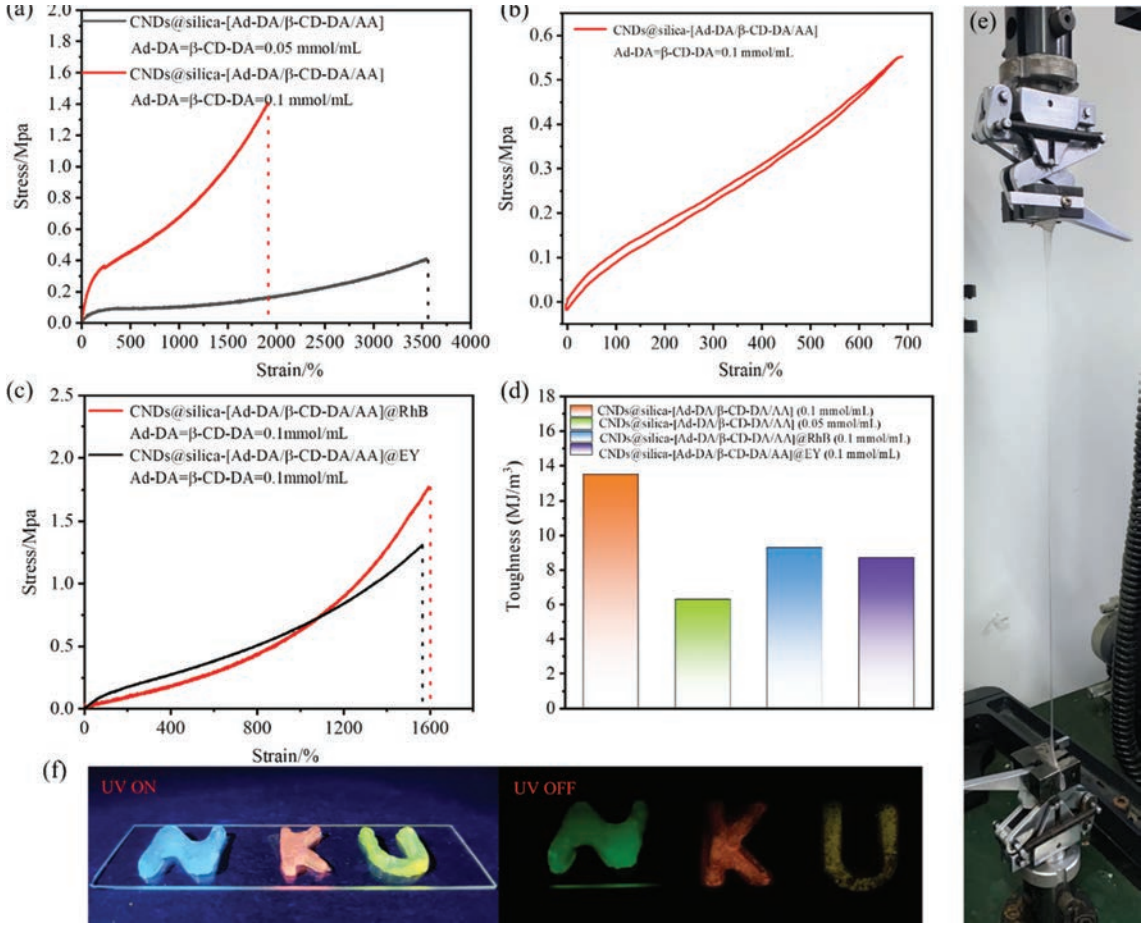

Fig. 3. (a) Tensile stress-strain curves of hydrogels with different concentrations of Ad-DA/β-CD-DA assembly. red, [Ad-DA] = [β-CD-DA] = 0.1 mmol/mL, [AA] = 3.4 mmol/mL; black, [Ad-DA] = [β-CD-DA] = 0.05 mmol/mL, [AA] = 3.4 mmol/mL. (b) Tensile loading-unloading curves of hydrogels at strain of 700% ([Ad-DA] = [β-CD-DA] = 0.1 mmol/mL, [AA] = 3.4 mmol/mL). (c) Tensile stress-strain curves of hydrogels doped with EY and RhB ([Ad-DA] = [β-CD-DA] = 0.1 mmol/mL, [AA] = 3.4 mmol/mL). (d) The fracture energy of hydrogels with different concentrations of Ad-DA/β-CD-DA assembly. (e) Visual photos used to show the excellent ductility ([Ad-DA] = [β-CD-DA] = 0.1 mmol/mL, [AA] = 3.4 mmol/mL). (f) The photographs of "N", "K", "U" before and after 365 nm irradiation.

EY or RhB, which is 9.6 MJ/m^3 or 8.9 MJ/m^3 respectively, and the minimum fracture energy of the hydrogel with 0.05 mmol/mL concentration Ad-DA/β-CD-DA assembly is 6.3 MJ/m^3 (Fig. 3d). The stability of the hydrogel at 0.1 mmol/mL concentration Ad-DA/β-CD-DA assembly was further studied by rheological experiments. As depicted in Fig. S26 (Supporting information), with the increase of strain from 0.1% to 1000%, the storage modulus (G') is always greater than the loss modulus (G''). The frequency sweep curve shows that with the increase of frequency from 0.1% to 100%, G' and G'' gradually increase and remain substantially parallel, and G' is always much larger than G'' (Fig. S27 in Supporting information). These results fully demonstrate the high stability of the three-dimensional network of hydrogels and further indicate that whether or not dye molecules are doped in the hydrogel did not affect its gel properties. Furthermore, these hydrogels have the good processability and formability. By injecting these hydrogels into different letter molds to produce multicolor "NKU", as depicted in Fig. 3f, "N", "K" and "U" emit bright blue, red and yellow light respectively under the irradiation of a 365 nm UV lamp. After the excitation light source is removed, they showed long-lived green phosphorescence (N), red (K) and yellow (U) delayed fluorescence at room temperature. The luminescence results of this gel phase further verified that the supramolecular phosphorescent materials we constructed can effectively carry out light harvesting energy transfer with dyes to achieve multicolor spectral adjustment.

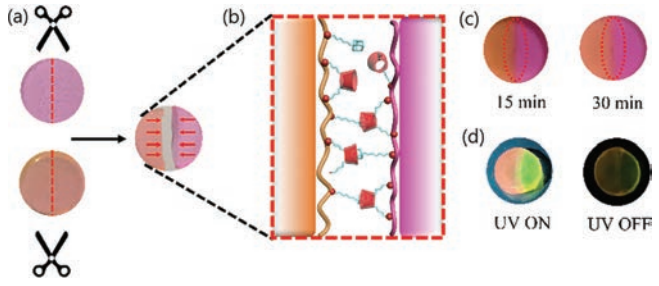

Fig. 4. (a) The digital images of circular hydrogels (pink, hydrogels doped with RhB; orange, hydrogels doped with EY). (b) Demonstration of the rapid self-healing property of hydrogels at 37 °C. (c) The images of an incision in the hydrogel over time. (d) The images of self-healing hydrogel before and after 365 nm irradiation.

Host-guest interaction is one of the most important interactions in supramolecular polymers. It is possible to spontaneously repair cracks or fractures of supramolecular materials to increase the service life through highly directional non-covalent interactions. In view of the unique properties of host-guest interaction of cyclodextrins in supramolecular self-healable materials, we also studied the self-healing capability of phosphorescent hydrogels. Firstly, two circular hydrogels doped with EY and RhB were prepared and cut into two pieces with scissors (Fig. 4a). Then, the two freshly obtained hydrogels were fixed with a clamp and incubate them

in an oven at 37 °C, and the changes of the hydrogels within 15–30 min were shown in Fig. 4c. It can be clearly seen that with the increase of incubation time, the cut cracks between the two hydrogels become blurred within 30 min, which indicates that effective self-healing may occur between the hydrogels. In order to validate the self-healing property, we use tweezers to clamp both ends for stretching. At this time, the recovered hydrogel could still withstand a certain stress and further withstand repeated shaking without breakage (Videos S5 and S6 in Supporting information). In the control experiments, the two pieces of hydrogel after coating the cut surface with free adamantane could not be "healed" to form the integrated hydrogel again (Video S6 in Supporting information). Interestingly, the two hydrogels emitted red and yellow delayed fluorescence respectively under 365 nm UV lamp after self-healing, and obvious afterglow was observed after the excitation light source was removed (Fig. 4d). Fig. 4b showed the mechanism of rapid self-healing of hydrogel. When the hydrogel was cut into two pieces, many free host molecules and guest molecules were distributed on the fracture surface. If hydrogels are tightly built together, it is easy to reorganize the cross-linking network through the host-guest interaction so as to achieve the rapid self-healing of the hydrogels. If two hydrogels use excessive free adamantane to coat the cutting surface before contacting each other, they will occupy the cyclodextrin cavity freely distributed on the hydrogel surface, so that the adamantane on the cutting surface cannot be well recognized, and the hydrogel will lose the ability of self-healing.

In conclusion, an organic-inorganic hybrid supramolecular phosphorescent hydrogel was successfully prepared by a simple strategy of *in-situ* thermal-initiated polymerization, resulting in one of the highest hydrogel phase phosphorescence lifetimes reported so far under ambient conditions. Long-lived singlet emission was achieved in hydrogel phase through an efficient TS-FRET, and the maximum lifetime of delayed fluorescence was 730 ms, which was rarely reported in hydrogel phase. Mechanical tests showed that the reversibility of host-guest interaction and energy-dissipation mechanism in hydrogels make them exhibit the strong tensile and fatigue resistant, and can rapid self-healing. This kind of hydrogel with excellent mechanical and phosphorescent properties is expected to be further applied in the material field.

Declaration of competing interest

The authors declare that they have no known competing financial interests or personal relationships that could have appeared to influence the work reported in this paper.

Acknowledgments

We thank National Natural Science Foundation of China (NNSFC, No. 22131008) and the Haihe Laboratory of Sustainable Chemical Transformations for financial support.

Supplementary materials

Supplementary material associated with this article can be found, in the online version, at doi:10.1016/j.cclet.2023.108644.

References

[1] X.H. Lin, J. Wang, B.B. Ding, et al., Angew. Chem. Int. Ed. 60 (2021) 3459–3463.
[2] Q.X. Dang, Y.Y. Jiang, J.F. Wang, et al., Adv. Mater. 32 (2020) 2006752.
[3] H.J. Yu, Q.Y. Zhou, X.Y. Dai, et al., J. Am. Chem. Soc. 143 (2021) 13887–13894.
[4] X. Zhang, Y.H. Cheng, J.X. You, et al., ACS Appl. Mater. Interfaces 14 (2022) 16582–16591.
[5] D.L. Wang, J.Y. Gong, Y. Xiong, et al., Adv. Funct. Mater. 33 (2023) 2208895.
[6] D.A. Xu, Q.Y. Zhou, X.Y. Dai, et al., Chin. Chem. Lett. 33 (2022) 851–854.
[7] C. Li, X. Li, Q. Wang, Chin. Chem. Lett. 33 (2022) 877–880.
[8] C.R. Wang, Y.Y. Gong, W.Z. Yuan, Y.M. Zhang, Chin. Chem. Lett. 27 (2016) 1184–1192.
[9] J. Yu, H. Wang, Y. Liu, Adv. Opt. Mater. 10 (2022) 2201761.
[10] S. Garain, B.C. Garain, M. Eswaramoorthy, et al., Angew. Chem. Int. Ed. 60 (2021) 19720–19724.
[11] Q. Peng, H.L. Ma, Z.G. Shuai, Acc. Chem. Res. 54 (2021) 940–949.
[12] H. Shi, W. Yao, W.P. Ye, et al., Acc. Chem. Res. 55 (2022) 3445–3459.
[13] E. Hamzehpoor, C. Ruchlin, Y.Z. Tao, et al., Nat. Chem. 15 (2023) 83–89.
[14] I. Bhattacharjee, S. Hirata, Adv. Mater. 32 (2020) 2001348.
[15] X.Y. Dai, M. Huo, X. Dong, et al., Adv. Mater. 34 (2022) 2203534.
[16] J.J. Guo, C.L. Yang, Y.L. Zhao, Acc. Chem. Res. 55 (2022) 1160–1170.
[17] W.H. Shao, J. Kim, Acc. Chem. Res. 55 (2022) 1573–1585.
[18] Y. Sun, Y. Chen, L.N. Jiang, et al., Adv. Opt. Mater. 10 (2022) 2201330.
[19] Y.L. Ning, J.F. Yang, H. Si, et al., Sci. China Chem. 64 (2021) 739–744.
[20] Y. Zheng, Z.H. Wang, J.W. Liu, et al., ACS Appl. Mater. Interfaces 14 (2022) 15706–15715.
[21] Y. Xia, C.F. Zhu, F. Cao, et al., Angew. Chem. Int. Ed. 135 (2023) e202217547.
[22] W.L. Zhou, Y. Chen, Q.L. Yu, et al., Nat. Commun. 11 (2020) 4655.
[23] S. Cai, Z. Sun, H. Wang, et al., J. Am. Chem. Soc. 143 (2021) 16256–16263.
[24] Y.F. Zhang, X.H. Chen, J.R. Xu, et al., J. Am. Chem. Soc. 144 (2022) 6107–6117.
[25] Y.F. Zhang, Y. Su, H.W. Wu, et al., J. Am. Chem. Soc. 143 (2021) 13675–13685.
[26] A. Roy, S. Wang, B. Meschede-Krasa, et al., Nat. Commun. 11 (2020) 11.
[27] Z.Z. Ding, C.L. Shen, J.F. Han, et al., Small (2022) 2205916.
[28] F. Liu, Z.Y. Li, Y. Li, et al., Carbon 181 (2021) 9–15.
[29] Y.C. Liang, S.S. Gou, K.K. Liu, et al., Nano Today 34 (2020) 100900.
[30] L. Feng, S.S. Jia, Y. Chen, Y. Liu, Chem. Eur. J. 26 (2020) 14080–14084.
[31] S.N. Kirmic Cosgun, D. Ceylan Tuncaboylu, Carbohydr. Polym. 269 (2021) 118278.
[32] Z.X. Liu, Y. Liu, Chem. Soc. Rev. 51 (2022) 4786–4827.
[33] M. Jain, B.J. Ravoo, Angew. Chem. Int. Ed. 60 (2021) 21062–21068.
[34] D. Zhang, W. Liang, J. Yi, et al., Sci. China Chem. 65 (2022) 1149–1156.
[35] Y. Rong, R. Liu, P. Jin, et al., J. Mater. Chem. A 11 (2023) 5895–5901.
[36] J. Li, C.D. Ji, B.Z. Lu, et al., ACS Appl. Mater. Interfaces 12 (2020) 36873–36881.
[37] S. Ikejiri, Y. Takashima, M. Osaki, et al., J. Am. Chem. Soc. 140 (2018) 17308–17315.
[38] J. Park, S. Murayama, M. Osaki, et al., Adv. Mater. 32 (2020) 2002008.
[39] Y. Kobayashi, A. Harada, H. Yamaguchi, Chem. Commun. 56 (2020) 13619–13622.
[40] K. Koyanagi, Y. Takashima, H. Yamaguchi, A. Harada, Macromolecules 50 (2017) 5695–5700.
[41] G. Sinawang, M. Osaki, Y. Takashima, et al., Chem. Commun. 56 (2020) 4381–4395.
[42] B.L. Zhang, J.H. He, M.T. Shi, et al., Chem. Eng. J. 400 (2020) 14.
[43] Z. Wang, Y. Ren, Y. Zhu, et al., Angew. Chem. Int. Ed. 57 (2018) 9008–9012.